Arabian Journal of Chemistry (2020) 13, 5262–5276

King Saud University

Arabian Journal of Chemistry

www.ksu.edu.sa
www.sciencedirect.com

ORIGINAL ARTICLE

Synthesis and characterization of a pH responsive and mucoadhesive drug delivery system for the controlled release application of anti-cancerous drug

R. Surya [a], Manohar D. Mullassery [a,*], Noeline B. Fernandez [a], Diana Thomas [a], Prasad S. Jayaram [b]

[a] Department of Chemistry, Fatima Mata National College, Kollam 691001, India
[b] National Centre for Biological Sciences, Bangalore, India

Received 28 August 2019; accepted 2 March 2020
Available online 12 March 2020

KEYWORDS

Chitosan;
Bentonite;
Paclitaxel;
Controlled drug delivery;
Mucin

Abstract In this work a novel pH sensitive composite, polyacrylamide grafted succinyl chitosan intercalated bentonite (AAm-g-NB/SC) was prepared as a drug carrier system for the controlled delivery of paclitaxel. Characterization of the drug delivery system was carried out using Fourier transform infrared spectroscopy (FTIR), X-ray diffraction (XRD), scanning electron microscopy (SEM), thermal analysis etc. The equilibrium swelling behaviour of the composite was studied and the result showed a maximum at pH 7.4. The in vitro drug release study of paclitaxel indicated that about 15.6% of drug release was found to be occurred at pH 1.2 within 16 h, whereas about 82.5% of drug release was occurred at the intestinal pH condition of 7.4. In vitro biocompatibility study was performed and the result showed good biocompatibility of the composite in the concentration range 6.25–100 μg/mL. The cytotoxicity assay was carried out in cancerous cell line of Human colorectal Adenocarcinoma. Mucous glycoprotein assay study showed that the drug delivery system having good apparent adhering property towards mucin. The investigation indicated that paclitaxel, an anticancer drug can be successfully entrapped in the AAm-g-NB/SC composite for the controlled and targeted delivery for colorectal cancer therapy.

1. Introduction

Efficient drug delivery and targeting is one of the major issues faced by bioactive drug molecules. Recent research on optimization of drug delivery systems which provide a defined dose, at a chosen rate and at selected time to a targeted biological site are quite impressive. The issues requiring continuous

* Corresponding author.
E-mail address: mdmullassery@gmail.com (M.D. Mullassery).
Peer review under responsibility of King Saud University.

ELSEVIER Production and hosting by Elsevier

https://doi.org/10.1016/j.arabjc.2020.03.005
1878-5352

research range from the fundamental understanding of the target and the practical constraints in designing the drug and the drug carrier systems to achieve targeted drug delivery. The influence of a drug in disease treatment is highly dependent on the ability of the therapeutic to selectively and effectively treat targeted cells and tissues while leaving other healthy parts of the body untouched. Researchers are constantly testing novel small molecule strategies to combat diseases. But relatively few of these drugs are used clinically due to low therapeutic windows for drug efficacy compared to drug related side effects. Drug delivery systems has therefore attracted wide attention in biomedical research due to their potential to significantly reduce the side effects of therapeutics, while making it possible to control the concentration and location of active drugs released in the body over long periods of time.

The use of biopolymer – clay mineral nanocomposite has attracted wide attention in pharmaceutical and biomedical field. The biopolymers such as cellulose, starch, alginic acid, chitosan etc are biodegradable (Abral et al., 2019). Like biopolymers, its composite with clay materials are also highly useful owing to their bio-compatibility, degradability and tunable mechanical properties. In order to attain a better therapeutic effect of drug molecules, the drug delivery systems should have the following characteristics such as targeting action and better gastrointestinal transit time (Akat et al., 2008; Jafarbeglou et al., 2016; Tiwari et al., 2012). The innermost layer of the human gastro intestinal tract called mucosa layer is responsible for the adsorption process which act as a protective barrier against the bacterial entry and its rapid multiplication (Dinakar, 2018; Rathee et al., 2011). Mucin, a glycolated protein is the building block of mucous membrane. The mucin has the binding property to hold the bioadhesive drug delivery system and allows the penetration of drug molecules into it. It is a better way of anti-cancerous drug release because increase in the retention of drug delivery system to the mucous layer may facilitate the administration of drug molecules to that targeted site and which will increase the mortality of cancer potent tissues (Helliwell, 1993).

Clay minerals that predominantly have properties governed by smectites are called bentonites. Montmorillonite is a major constituent of most bentonites (typically 80–90 wt%), the remainder being a mixture of mineral impurities including quartz, crystobalite, feldspar and various other clay minerals depending on the geological origin (Shin et al., 2016). This group of clay minerals has a dioctahedral or trioctahedral 2:1 layer structure, with isomorphous substitution that leads to a negative layer charge of <1.2 per formula unit (Asgari et al., 2017; He et al., 2014). The interlayer spacing varies between 10 and 15 Å and are generally dependent on the nature of exchangeable cation and the relative humidity (Tetsuka et al., 2018). Montmorillonite systems are dioctahedral smectites with layer charges predominantly in octahedral and tetrahedral sites, respectively. The general formula of the montmorillonite group can be represented as $(M_x^+)^{ex}[(Si_8)^{tet}(M(III)_{4-x}M(II)_x)^{oct}O_{20}(OH)_4]x-$, where M^+ is the exchangeable cation present in the interlayer (e.g. Na^+) and M (III) and M (II) are non-exchangeable octahedrally trivalent and divalent cations (e.g. Al^{3+} and Mg^{2+}) respectively, and the layer charge is $0.5 < x < 1.2$. (Bertuoli et al., 2014) The surface property of bentonite can be enhanced by introducing silylated amino functional groups. Tuneable pore size is a pre-requisite for the successful loading and the release of the drug, the release kinetics may be slower than expected if the pore size of the carrier is very small (Sörensen et al., 2009). However, in the development of clay based sustained release formulations, modulation of surface properties is essential to improve its affinity for bioactive molecules (Surya et al., 2019, Jafarbeglou et al., 2016). Further, clay minerals and polymers were often used in pristine form as a single drug carrier, they did not meet all the requirements. Therefore the preparation of polymer-layered silicate composite offered the possibility of improving the properties of individual components.

Chitosan is an excipient that could improve the dissolution rate of hydrophobic drugs and is a good adsorption enhancer (Khan, 2019; Aycan and Alemdar, 2018). Chitosan is a natural cationic polymer of N-acetylglucosamine and D-glucosamine monomer unit derived from chitin. Chitosan is a biodegradable, biocompatible, mucoadhesive and non-toxic biopolymer (Feng et al., 2015; Yan et al., 2006). Many of the researches utilize these specialties of chitosan in order to develop drug delivery system. But one of the main drawbacks of chitosan is its less solubility in aqueous medium at physiological pH conditions (Golyshev et al., 2015). To improve the hydrophilicity of chitosan, it is essential to convert them into different kinds of derivatives such as N-maleoyl modified chitosan, N-acyl modified chitosan, quarternized form of chitosan, PEGylated derivative of chitosan etc (Anirudhan and Sandeep, 2011; Mukhopadhyay et al., 2014).

In the present study, the cationic biopolymer chitosan was modified with succinic anhydride and intercalated between the laminar spacing of the clay. Further, it was polymerized using acrylamide monomer units, ammonium persulphate as the free radical initiator, EGDMA as the cross linking agent and AIBN as the accelerator for the controlled release of paclitaxel (PTX) an anti-cancerous drug for the colorectal cancer therapy.

2. Experimental

2.1. Materials

Bentonite clay was procured from Ashapura Clay Mines, Gujarat, India, having the physical parameters given in Table 1. Chitosan (CTS) (200–600 mPa.s, 0.5% in 0.5% acetic acid at 20 °C) and the crosslinking agent ethyleneglycoldimethacrylate (EGDMA) (greater than 0.97%) were purchased from Tokyo Chemical Industry, Japan. EGDMA is a derivative of ethylene glycol. Acrylamide (AAm) (99.0%) was received from Merck Life Solence Pvt. Ltd., India. Ammonium per sulphate (APS) was purchased from Merck Speciali-

Table 1 Physicochemical properties of Na- bentonite.

Parameters	Magnitude
d (0 0 1) values (Å)	14.4
Surface area ($m^2\ g^{-1}$)	39.7
Apparent density ($g\ mL^{-1}$)	1.7
Porosity ($mL\ g^{-1}$)	0.39
Cation exchange capacity ($meq\ g^{-1}$)	0.69
Zero point charge (pH_{zpc})	7.8
Particle size (mm)	0.096

ties Pvt. Ltd., India. APS is a free radical initiator of polymerisation reaction. Acetone (99.0%) and α, α-azobisisobutyronitrile (AIBN) (98.0%) were procured from Spectrochem. Pvt. Ltd (India). Paclitaxel (99.0%) was purchased from Alfa Aesar, England. MTT (3-(4, 5-dimethylthiazol-2-yl)-2, 5-diphenyltetrazolium bromide) having the molecular formula $C_{18}H_{16}BrN_5S$, was purchased from Himedia, India). DLD1 (Human Colorectal Adenocarcinoma) cells was initially procured from National Centre for Cell Sciences (NCCS), Pune, India and maintained Dulbecco's modified Eagles medium, DMEM Sigma Aldrich, USA. The pH of the medium was adjusted using phosphate and citrate buffer. Distilled water with the specific conductivity < 1 μ Scm^{-1} was used throughout the study.

2.2. Methods

2.2.1. Synthesis of drug delivery system involves the following steps

2.2.1.1. Succinyl modification of chitosan by homogeneous method. Succinyl modified chitosan (SC) was synthesized according to an earlier reported procedure (Golyshev et al., 2015; Mukhopadhyay et al., 2014; Yan et al., 2006). Briefly, about 2 g of succinic anhydride (SA) was dissolved in 40 mL DMSO, to this added same amount of chitosan. The reactor was placed at the temperature condition of ~65 °C for 6 h. The precipitate was filtered and poured into excess ethanol for 1 h at normal temperature condition. After that the pH was adjusted to alkaline (10–12) using 1 M NaOH solution. The precipitate was filtered, washed and re-precipitated using acetone. The final product was dried under vacuum condition.

Similar findings were also reported by Anirudhan et al 2011. They reported the applicability of maleoylchitosan (MACTS) intercalated montmorillonite, which was further grafted using 2-Acrylamido-2-methylpropane sulfonic acid, with KPS as the free radical initiator and N,N-methylenebisacrylamide (MBA) as a crosslinking agent.

2.2.1.2. Intercalation of sodium bentonite with succinyl chitosan (SC/NB). An aqueous solution of about 1 g succinyl chitosan was taken and the pH was adjusted to 3.5 using 1 M HCl. Then it was added slowly to 2 g of sodium bentonite which was already dispersed in 100 mL distilled water. Stirred the reacting mixture for about 6 h by keeping the temperature nearly 60 °C. Finally, it was washed with distilled water till it reached the neutral pH (pH ~7), and dried.

2.2.1.3. Synthesis of polyacrylamide grafted succinylchitosan intercalated bentonite (AAm-g-NB/SC). About 1.5 g of acrylamide was dissolved in 50 mL water and about 3.0 g of NB/SC was mixed. The mixture was stirred continuously for 10 h. Calculated amount of initiator (ammonium peroxosulphate) and the crosslinking agent ethylene glycol methacrylate were added and stirred for 10 min and placed the mixture in a water bath and maintain the temperature to 70 °C for 12 h for the thermal initiation. After that the pH of the resulting product was adjusted to neutral (pH = 7) by using 1 M NaOH solution. The resulting product was dehydrated using methanol and the excess methanol was removed from the product. The product was then dried and powdered to suitable size (Mukhopadhyay et al., 2014).

2.3. Swelling nature of the composite

The swelling of composite in different physiological pH conditions was studied to evaluate the pH responsive nature of the composite. Calculated amount of the composite was taken in a dialysis bag and immersed in solution with variable pH of 1.2, 6.8 & 7.4 for 6 h. The composite was taken out at specific intervals and wiped using tissue paper and the weight of composite was measured using electronic balance. The % of swelling can be calculated according to Eq. (1).

$$\text{Swelling (g/g)} = \frac{W_{wet} - W_{dry}}{W_{dry}} \tag{1}$$

2.4. Drug encapsulation study

About 0.1 g of the composite was immersed in ~ 0.117 mol/L of paclitaxel in DMSO. The entire solution was shaken constantly for 10 h and it was washed with deionized water to remove the loosely bound drug molecules. The drug loading capacity and the encapsulation efficiency can be determined by the following equations.

$$\text{Encapsulation efficiency (EE)} = \frac{\textit{Concentration of the drug encapsulated in the composite}}{\textit{Total concentration of the drug}} \times 100 \tag{2}$$

$$\text{Drug loading efficiency (DLE)} = \frac{\textit{Concentration of drug in the composite}}{\textit{Total concentration of the composite}} \times 100 \tag{3}$$

2.5. In-vitro release study and the mathematical modeling

About 0.1 g of the PTX-Loaded DDS was immersed in 250 mL of physiological buffer solutions of pH 1.2 and 7.4 and placed in a water bath shaker by maintaining the temperature at 37 °C. At specific intervals the aliquot was taken out and the amount of drug release was measured using the UV–Visible Spectrophotometer at 227 nm.

$$\%\ \text{of drug release} = \frac{\textit{Amount of drug release}}{\textit{Total amount of drug loaded}} \times 100 \tag{4}$$

2.6. Mucous glycoprotein assay (Mucin assay)

In order to measure the binding capacity of the composite to mucin, taken about 20 mg of the composite into an aqueous solution of mucin (variable concentration of mucin from 0.1 to 1 mg). Shaken constantly for 30 min at a temperature of 37 °C and centrifuge the dispersion. The concentration of

non-adhered mucin (free mucin) was measured by using the UV–Visible spectrophotometer at a wavelength of 555 nm (Feng et al., 2015).

2.7. Biocompatibility assay

The cell line, Human Colorectal Adenocarcinoma (DLD1) was cultured in 25 cm^2 tissue culture flask with DMEM supplemented with 10% FBS, L-glutamine, sodium bicarbonate (Merck, Germany) and antibiotic solution containing: Penicillin (100 U/mL), Streptomycin (100 μg/mL), and Amphotericin B (2.5 μg/mL). Cultured cell lines were kept at 37 °C in a humidified 5% CO_2 incubator (NBS Eppendorf, Germany). The viability of cells was evaluated by direct observation of cells through Inverted phase contrast microscope and followed by MTT assay method.

About 15 mg of MTT (Sigma, M−5655) was reconstituted in 3 mL PBS until completely dissolved and sterilized by filter sterilization. After 24 h of incubation period, the sample content in the wells were removed and 30 μL of reconstituted MTT solution was added to all test (100 μg, 50 μg, 25 μg, 12.5 μg, 6.25 μg in 500 μL of 5% DMEM) and cell control wells, the plate was gently shaken well, then incubated at 37 °C in a humidified 5% CO_2 incubator for 4 h. After the incubation period, the supernatant was removed and 100 μL of MTT solubilization. Solution (Dimethyl sulphoxide, DMSO, Sigma Aldrich, USA) was added and the wells were mixed gently by pipetting up and down in order to solubilize the formazan crystals. The absorbance values were measured by using microplate reader at a wavelength of 540 nm.

The percentage of growth inhibition was calculated using the formula:

$$\%\ \text{of viability} = \frac{Mean\ OD\ of\ sample}{Mean\ OD\ of\ control} \times 100 \quad (5)$$

2.8. Determination of apoptosis by acridine orange (AO) and ethidium bromide (EtBr) double staining method

After treatment with sample at a final concentration of 161.67 μg/mL (LC 50 Concentration) for 24 h, the cells were washed by cold PBS and then stained with a mixture of AO (100 μg/mL) and EtBr (100 μg/mL) at room temperature for 10 min. The stained cells were washed twice with 1X PBS and observed by a fluorescence microscope in a blue filter of fluorescent microscope (Olympus CKX41 with Optika Pro5 camera).

2.9. Flow cytometry analysis

Analysis of DNA content and cell cycle distribution using cell cycle kit can be done by flow cytometry. DLD1 (Human colorectal Adenocarcinoma) cells were cultured as per standard procedures described earlier and treated with LC 50 concentration of sample (161.67 μg/mL) for 24 h. The cell sample was transferred to a 50 mL conical flask. The minimum recommended number of cells for fixation in a tube was 1 × 106 cells. The samples were then centrifuged at 3000 rpm for 5 min. The supernatant was removed without disturbing the pellet. After centrifugation, the cell pellet forms either a visible pellet or a white film on the bottom of the tube.

Appropriate volume of PBS was added to each tube (1 mL of PBS per 1×10^6 cells) and the contents were mixed by pipetting several times or gently vortexing. The cells were centrifuged at 3000 rpm for 5 min. The supernatant was discarded without disturbing the cell pellet, leaving approximately 50 μL of PBS per 1 × 106 cells. Suspend the pellet in the residual PBS by repeated pipetting several times. The suspended cells were added drop wise into the tube containing 1 mL of ice cold 70% ethanol while vortexing at medium speed. Cap and freeze the tube at −20 °C.

2.10. Staining of cell cycle

After overnight incubation, the samples were centrifuged at 3000 rpm for 5 min at room temperature. The supernatant was removed and 250 μL PBS was added to the pellet. Then the centrifugation was done again at the same rpm and time. The pellet was taken after discarding the supernatant and 250 μLof cell cycle reagent was added. This was incubated at dark for 30 min (which is light sensitive) and this was analysed using a Flow Cytometer. Gating was performed with reference to untreated control cells and samples were analysed.

2.11. Statistical analysis

All the results were expressed as mean ± standard deviation (SD). Statistical analysis was performed with origin 8.0 (Origin –Lab Corporation- USA).

3. Result and discussion

Even though chitosan (CTS) is a cationic polysaccharide having mucoadhesive properties, its water insolubility becomes a main barrier against biomedical applications. The solubility can be enhanced by the conversion of chitosan into its derivatives (Anirudhan and Sandeep, 2011). Succinyl chitosan was synthesised by introducing the succinyl group to the N-terminal of glucosamine unit in the chitosan. The zeta potential of succinyl chitosan at neutral pH condition was found to be negative (-20 mV), and at acidic pH conditions the zeta potential was positive (+9.34 mV) which was due to the presence of both –COO– and $–NH_2$ groups.

Succinyl chitosan was further intercalated in the layered clay. Sodium metal ions and other cationic species are the exchangeable ions in the clay. In acidic pH conditions the cationic exchange between the polycations (Na^+, Ca^{2+}) with the succinyl chitosan was possible. Because, at lower pH succinyl chitosan can attain cationic behaviour (zeta potential = +9.34 mV).

The final step in the synthesis of composite was the polymerisation step by using APS as the initiator and EGDMA as the crosslinking agent. The *insitu* polymerisation of succinyl chitosan (SC) and the acrylamide monomer unit was produced by the sulphate radical (by the thermal decomposition of persulphate). The sulphate radical abstract a hydrogen from the functional group of succinyl chitosan (–COOH, –OH or $–NH_2$) to form a macro radical. This radical may undergo copolymerisation with the acrylamide units and are further cross linked by EGDMA (Scheme 1). The copolymer formed exists in the crosslinked structure. The final composite formed

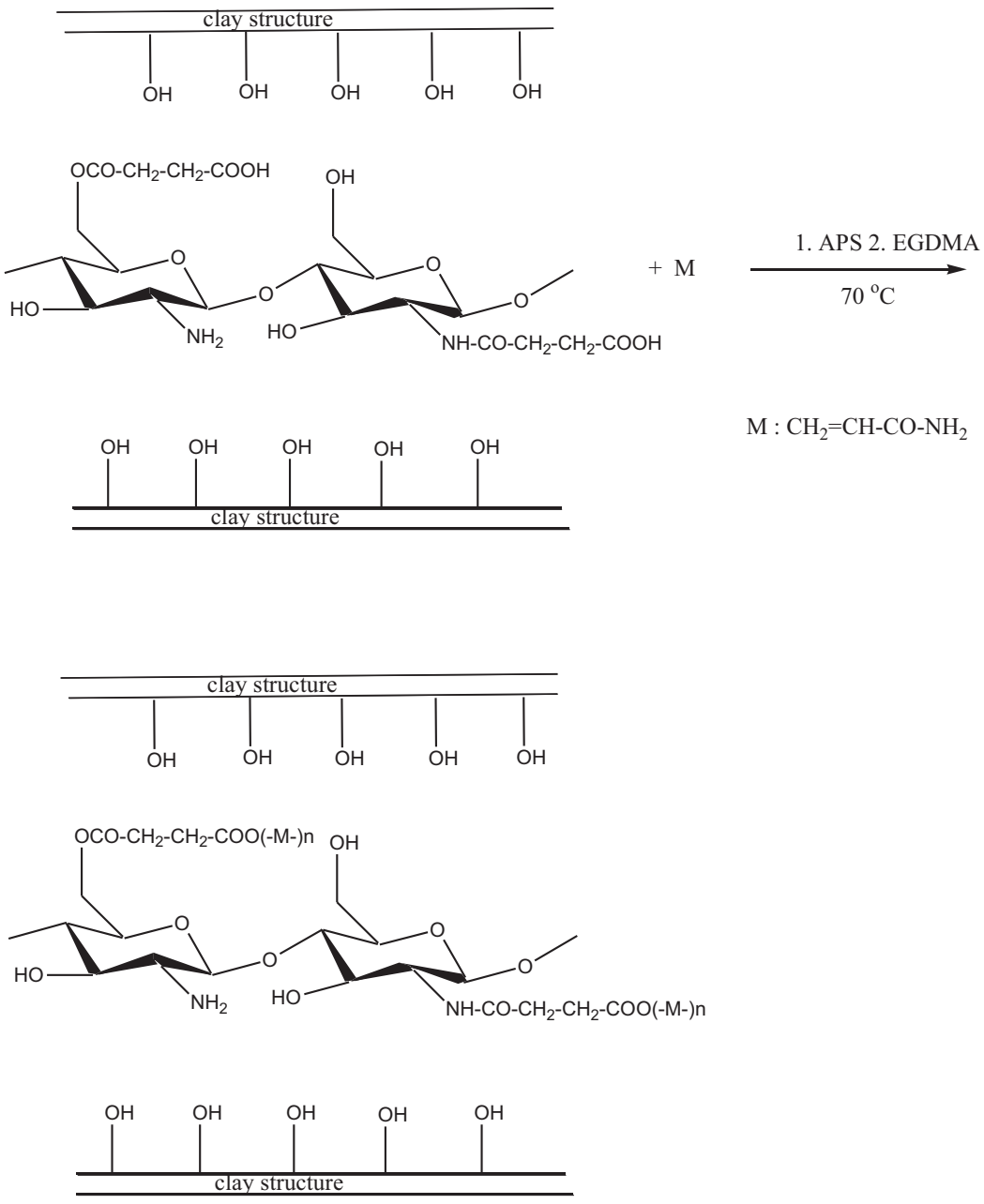

Scheme 1 The proposed reaction scheme for the synthesis of AAm-g-NB/SC.

have zeta potential of −47.4 mV which indicates the better stability of the drug delivery system.

3.1. Swelling study

In the case of polymeric composites, the swelling property had a prominent role in the release kinetics. The absorption of water molecule by a material is highly depends on the hydrophilic groups such as hydroxyl group (Halimatul et al., 2019; Ilyas et al., 2018a). The present work mainly focused on the pH responsive release study of the drug, therefore the swelling of the composite was studied by considering the pH as a parameter. Three different pH of 1.2, 6.8 and 7.4 were taken for the swelling studies in order to mimic the gastric and intestinal pH conditions (Fig. 1).

At the pH of 1.2 most of the carboxylate groups were appeared as protonated (–COOH) and there was a possibility for hydrogen bond interaction and may lead to the shrinkage of the composite (Li et al., 2007). As the pH was changed from acidic to neutral conditions the swelling was found to be increased due to the existence of deprotonated carboxylate anions, which might cause the anion-anion repulsion and the composite was found to be swollen (Pourjavadi and Mahdavinia, 2006). Among these three selected pH conditions,

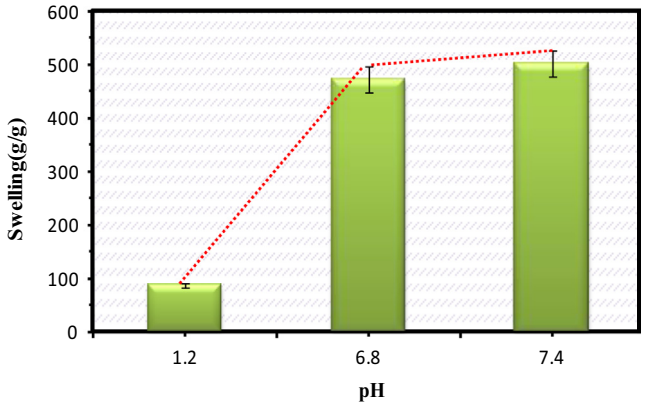

Fig. 1 Swelling profile of the drug delivery system at different pH environments.

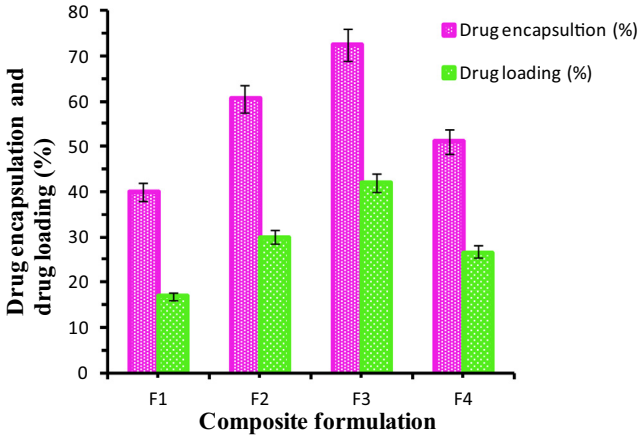

Fig. 2 The drug encapsulation and drug loading % of the composite having the different formulations.

the maximum swelling was found to be occurring at the intestinal pH conditions. In both the pH conditions of 6.8 and 7.4 the swelling percentage was found to increase with increase in pH. Swelling of the composite may take place at a pH greater than the pKa of the composite (Pourjavadi et al., 2008). Chitosan, the major component of the composite has the pKa value of 6.5 which favoured the swelling of the composite at pH 7.4 (Torres et al., 2007).

During the study it was ascertained that the amount of monomer unit (AAm) and the crosslinking agent (EGDMA) had direct influence in the swelling property and the release kinetics. Four different formulations of DDS was synthesised by varying the amount of AAm and EGDMA.

The optimum condition for the maximum swelling of the composite is presented in Table 2. Even at different pH conditions the influence of the crosslinking agent and the monomer on swelling profile was observed. The equilibrium swelling was found to be occurring within 1 h.

3.2. Drug encapsulation studies

Encapsulation efficiency is the total amount of drug entrapped into the drug carrier system whereas the % of drug loading indicates the amount of drug loaded per unit weight of the drug carrier system. The theoretical drug loading percentage was obtained as 42% and the % of encapsulation efficiency was found to be 72.5%. The formulation of composite has influence in the encapsulation of drug molecules within the drug delivery system (Fig. 2).

The % of encapsulation was found to vary with varying the concentration of the monomer and the crosslinking agent. The maximum encapsulation efficiency was observed for F_3 (Formulation 3) as indicated in Table 2. With the increase in monomer concentration the encapsulation was found to be increased up to a limit. This may be due to the diffusion of the drug molecules into the polymeric matrix. But as the concentration of AAm increased from 0.2 g to 0.4 g, the encapsulation was found to be decreased doubly. This can be explained as follows:(i) there is a possibility for homo-polymerisation of the monomer units which may retard the entry of the drug molecules (ii) the increasing proportion of the sol in the composite may lead to the decrease in encapsulation efficiency (Anirudhan and Sandeep, 2011). Similarly as the amount of crosslinking agent increases from 0.2 to 0.4 g, the encapsulation gets decreased due to the rigidity in the structure. The swelling pattern of the composite for various formulations at different pH were shown in Fig. 3.

3.3. FT-IR

Fig. 4 represents the FT-IR spectra of chitosan (CTS), succinyl chitosan (SC), succinyl chitosan intercalated clay (SC/NB), DDS (AAm-g-SC/NB) and PTX loaded DDS (PTX-L-AAm-g-SC/NB). In chitosan, the basic bands were observed at 3418 cm^{-1} which was due to the O-H and N-H stretching vibrations. The bands found at 2920 and 2854 cm^{-1} may due to the C-H stretching vibrations. The bands at 1650 cm^{-1} was due to the NH_2 deformation. And also the presence of bands at 1151 cm^{-1} and 1095 cm^{-1} were due to the bridged oxygen stretching and C-O stretching vibrations respectively. These results indicate the presence of the hydroxyl, amino group and the polymeric form of chitosan via glycosidic linkages (Kumar and Koh, 2012).

Table 2 Formulation parameters in the synthesis of drug delivery system.

Sample code	Amount of SC/N[a] (g)	Amount of the monomer AAm (g)	Amount of the cross-linker EGDMA (g)	Swelling in aqueous medium (g/g)
F_1	1.0	0.2	0.2	378
F_2	1.0	0.2	0.4	402
F_3	1.0	0.4	0.2	456
F_4	1.0	0.4	0.4	391

[a] Insert SC/NB instead of SC/N

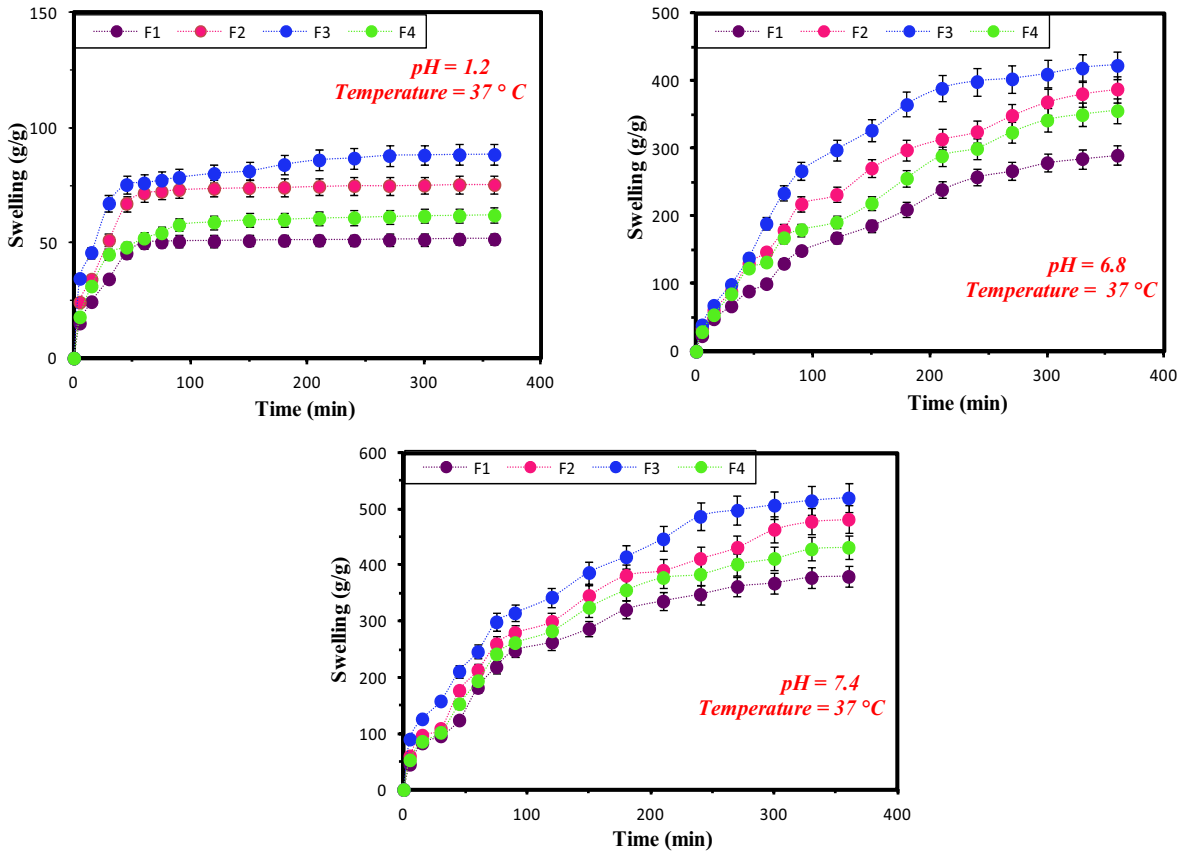

Fig. 3 The Swelling pattern of the composite for variable formulations at pH 1.2, 6.8 and 7.4.

In succinyl chitosan, the band at 1418 cm^{-1} indicates the symmetric stretching of carboxylate groups. This can be considered as an evidence for the succinyl modification of chitosan. The appearance of weak band at 1595 cm^{-1} indicates the $–NH_2$ bending vibration and the band at 1562 cm^{-1} indicates the presence of secondary amine group (Li et al., 2007). The band at 1014 cm^{-1} in bentonite represent the Si-OH (Bertuoli et al., 2014), which was found to be existing with decrease in intensity in SC/NB. This can be explained based on the participation of –OH group during the intercalation. The bands present at 3470 cm^{-1} in SC/NB was found to be decreased in wave number to 3430 cm^{-1} in the final composite which may due to the introduction of the monomer units onto the interlayer of clay during the polymerisation. In PTX, the bands at 3478–3300 cm^{-1} and 2975–2884 cm^{-1} represent the N-H stretching vibration and C-H stretching vibration (both asymmetric and symmetric) respectively. The band at 1647 cm^{-1} indicate the amide bond and band at 1734 cm^{-1} represents the C = O stretching vibrations. The bands at 1647, 1073, 965 and 708 cm^{-1}represent the aromatic moiety (Martins et al., 2014). After the drug loading the intense bands of the drug are getting disappeared and the spectrum shows more similarity with the drug delivery system. This indicates that there was no chemical interaction as occurred between the drug and the drug carrier system.

3.4. XRD

XRD is a common method to investigate the crystalline nature and the composition of advanced materials (Niu et al., 2019a, b). The XRD characterisations of SC, NB, SC/NB, AAm-g-SC/NB and PTX-L- AAm-g-SC/NB are shown in Fig. 5. The crystallinity of the composite can be understood from the sharpness of the peak (Ahmad et al., 2019). The XRD pattern of chitosan showed a peak at 2θ = 10° and another at 2θ = 20°. The peak at 10° was due to the crystalline nature of the chitosan (Mukhopadhyay et al., 2014). In succinyl chitosan the peak at 10° was disappeared and the reflection of peak at 20° was decreased. This was due to the breakage of intermolecular hydrogen bonds between $–NH_2$ and –OH group due to succinyl modification. The crystalline nature of chitosan was disrupted following the succinyl modification.

The XRD pattern of NB showed a characteristic (0 0 1) reflection peak at 2θ = 6.89° corresponding to the d-spacing value of 13.02 Å (Bertuoli et al., 2014). The interaction of SC with the bentonite layer caused the increase in interplanar distance to 19.9 Å. This increase in basal spacing clearly suggests the intercalation of SC onto NB. After the polymerization the d- spacing was again increased to 24.6 Å was explained due to the entry of monomer units and its polymerization within the clay interface.

3.5. SEM analysis

The SEM images of Na-B, SC/NB, DDS and PTX-L-DDS are shown in Fig. 6. The morphology of each compound can be distinguished from the figure. As reported earlier bentonite has corn flakestructure (Mullassery et al., 2018). After the intercalation the morphology was changed to laminar type with enlarged particle size. This may due to the intercalation

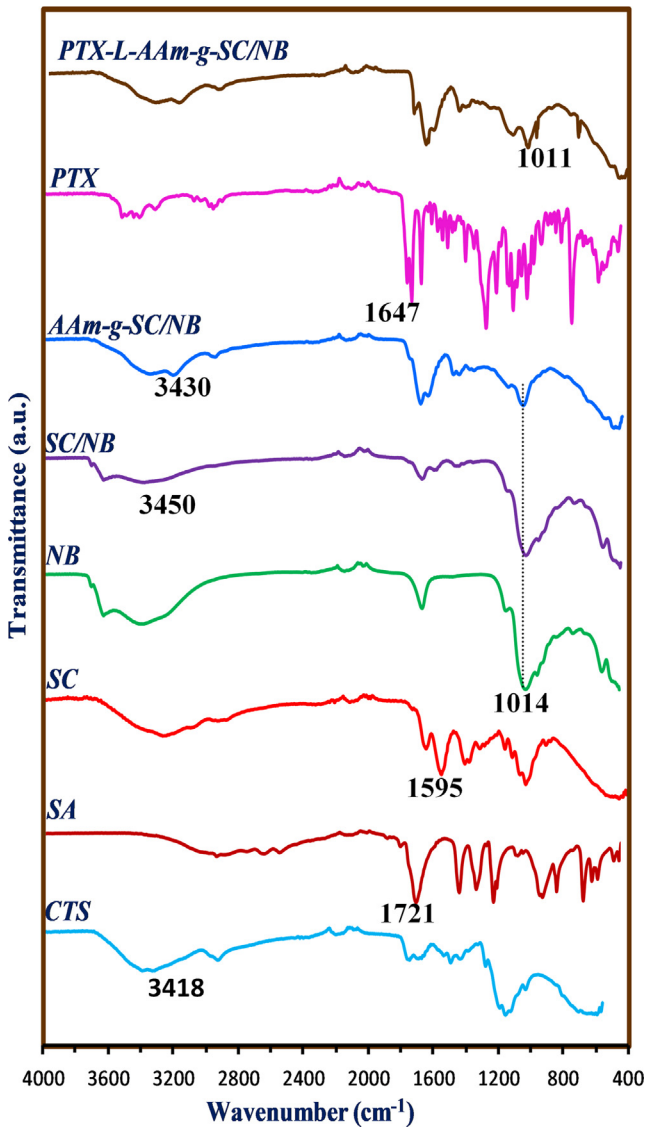

Fig. 4 FT-IR spectra of CTS, SA, SC, NB, SC/NB, AAm-g-SC/NB, PTX and PTX loaded AAm-g-SC/NB.

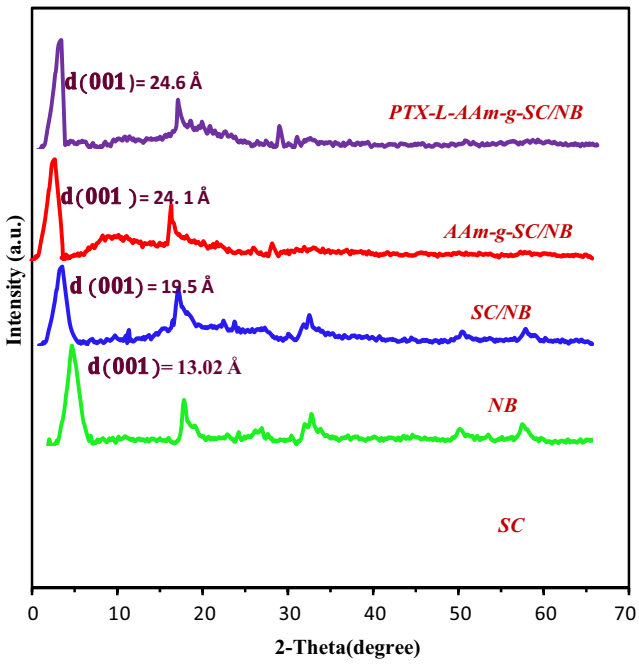

Fig. 5 XRD of SC, NB, SC/NB, AAm-g-SC/NB and PTX-L-AAm-g-SC/NB.

of succinyl chitosan with in the laminar layers of bentonite clay. After the polymerisation, the drug delivery system was found to be occurring with more uniform porous morphology. This was very important for the entry of the drug molecules with in the gallery of DDS. After the loading of paclitaxel, porous nature was slightly reduced and the DDS appear with a comparatively homogeneous morphology. This is a clear proof for the encapsulation of the drug molecules within the DDS.

3.6. TEM and DLS analysis

The hydrodynamic particle size of the composite was obtained from DLS (Fig. 7). By using the DLS analysis, it was possible to determine the particle size variation of the composite at different pH conditions. It was found that the hydrodynamic particle size gets increased with increase in pH. The particle size at pH 1.2 was found to be 169.9 which was greater than the size obtained from the TEM analysis. And it was found that the particle size increased to 298.5 nm at pH = 7.4. This is also an indication for the pH responsive swelling nature of the drug delivery system. After the drug loading it was found that the particle size of the drug delivery system have a noticeable increase from 168.6 nm to 202 nm. It can be considered as a positive evidence for the successful drug encapsulation.

The morphology of the materials can be understood from the TEM images (Niu et al., 2018). The TEM image of the composite is shown in Fig. 8. From the TEM images it was found that the clay layers are stacked as parallel having variable sizes, indicated the intercalation mechanism. This results again proved the intercalation of clay–polymer as evident from the XRD data (Mansa and Detellier, 2013). The overall dispersion of clay in polymer can be understood from the low magnification, and the intercalated or exfoliated structure can be understood from the high magnification images of TEM. Since silicates layer are composed of heavier elements (Al, Si and O) than the surrounding matrix, they appeared darker in bright field images. The dark color indicates the clay and the colorless part shows the polymeric matrix.

3.7. Thermo gravimetric analysis

The thermogravimetric analysis was used to investigate the thermal stability of composites with respect to weight loss due to increase in temperature (Ilyas et al., 2018b). In the TGA of Na-B, there are two weight loss as found in the figure (Fig. 9). The weight loss below 150 °C attributes to the evaporation of water molecules. And the second weight loss between 450 °C −700 °C was due to the removal of the structural –OH groups from the edges of clay. In succinyl chitosan intercalated bentonite the weight loss events were similar to

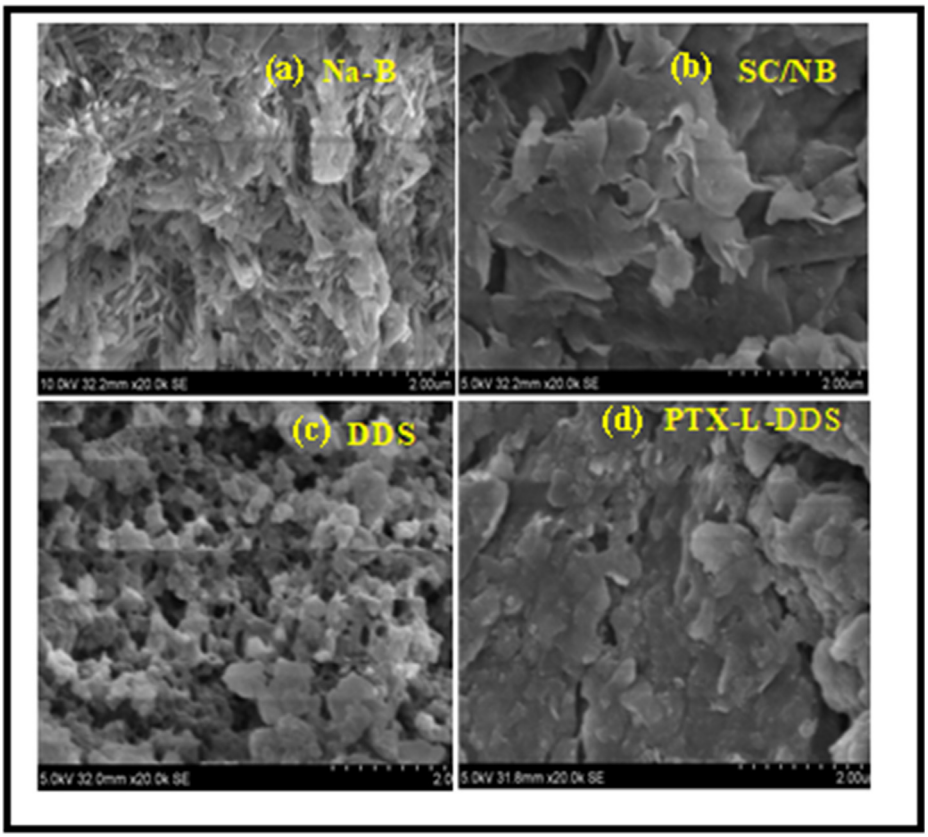

Fig. 6 FE-SEM images of a) Na-B, b) SC/NB, c) DDS (AAm-g-NB/SC) and d) PTX-L-DDS (PTX-L-AAm-g-NB/SC).

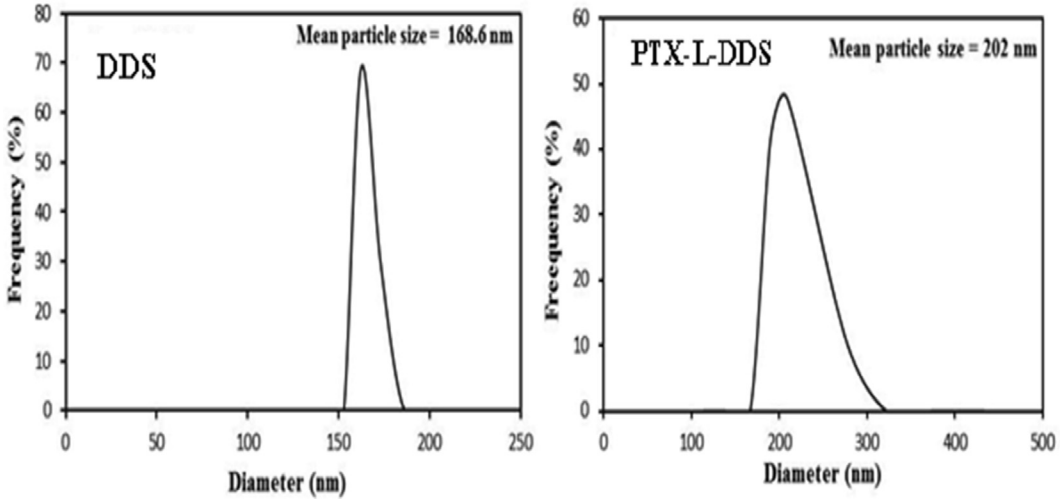

Fig. 7 DLS of AAm-g-NB/SC and PTX-L-AAm-g-NB/SC.

that observed for bentonite clay at temperature below 150 °C. This was explained for the removal of free water molecules. The degradation of succinyl chitosan intercalated clay was started from 200 °C. The degradation between 250 °C −500 °C may due to the removal of intercalated succinyl chitosan from the interlayer of clay. Similar to the bentonite clay the weight loss for SC/NB above 500 °C attributes to the –OH group removal from the edges. The weight loss difference between the pure bentonite and that of the succinyl chitosan intercalated bentonite is a good evidence for the intercalation. In the case of DDS about 50% weight loss was found between the temperature range of 200 °C – 400 °C which may due to the breakage of polymerised and cross-linked succinyl chitosan. In the case of PTX-L-DDS, same trend was occurring. But the total weight loss of PTX-L-DDS was found to be less than that of DDS can be considered as an evidence for the higher thermal stability of drug in the drug delivery system.

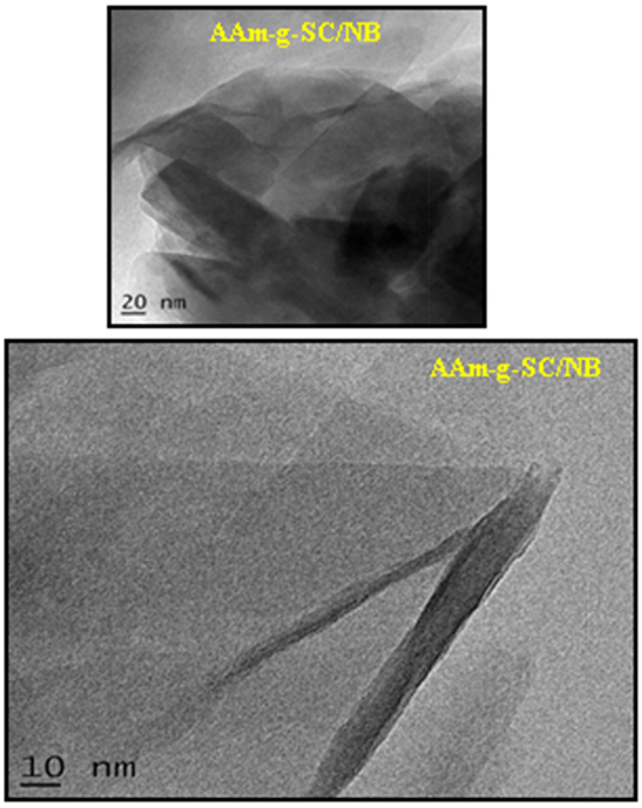

Fig. 8 TEM image of AAm-g-SC/NB.

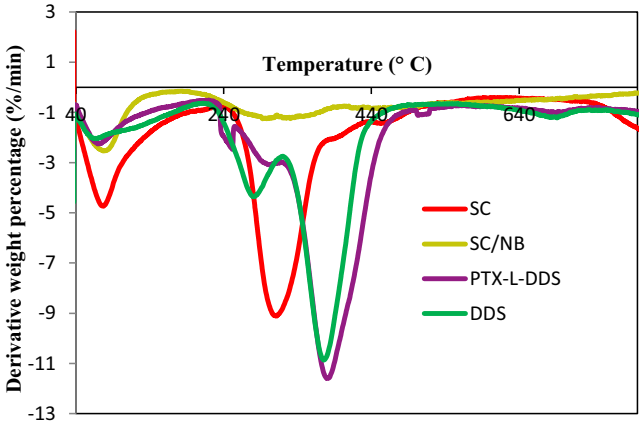

Fig. 9 DTG analysis of Na-B (NB), Clay-SC (SC/NB), DDS (AAm-g-SC/NB), PTX-L-DDS.

3.8. In vitro release study

The release study of PTX was carried out at simulated gastric condition of pH = 1.2 and simulated intestinal pH of 7.4. In order to mimic the pH variation of gastro intestinal tract the release study was carried out in two phases. For the first 2 h the release profile was evaluated at pH 1.2, after that the same material was poured in the physiological buffer of pH = 7.4 (Fig. 10).

About 15.6% of drug release was found to be occurred at pH 1.2 within 16 h, whereas about 82.5% of drug release was occurred at the intestinal pH condition of 7.4. This indicates the protective effect of the drug delivery system from the acidic gastric pH conditions. The time taken for the 50% of drug release (t_{50}) was found to be 6 h. This means the release of drug occur in a controlled manner without a burst release. In the basic pH condition, the carboxylic acid gets deprotonated and also the electrostatic interaction between the hydrophilic functional groups get decreased which led to the swelling of the matrices and the release of drug molecules to the solvent media.

According to the earlier studies the successful release of the drug molecules at pH = 7.4 is ideal for the release of drug in the large intestine, colon and rectal mucosa, each part possesses different emptying times (Amidon et al., 2015).

Release kinetics mechanism can be explained by Peppas kinetic model

$$\frac{M_t}{M_\infty} = \mathrm{Kt}$$

M_t = amount of drug release at time t
M_∞ = amount of drug release at infinity
K = Release constant
n = Release exponent

The parameter 'n' can explain the type of release mechanism. If n < 0.43, release of drug is purely due to the diffusion mechanism. If 0.43 < n < 0.85, the release kinetics is controlled by both swelling and diffusion mechanism and if n greater than 0.85, the release of drug molecules are purely due to the swelling of the composite (Siepmann and Peppas, 2012).

3.9. Mucous glycoprotein assay

Mucous glycoprotein assay is an *in-vitro* method to find out the capability of the drug delivery system to adhere onto mucous membrane. Mucin is actually a protein produced by the mucus layer. It is composed of sialic acid, hexosamine and sugar with large number of hydroxyl groups (Feng et al., 2015). Due to the presence of this functional group it is possible to form hydrogen bond interaction with the functional groups of drug delivery system.

During the analysis ~20 mg of sample was added to the aqueous solution of mucin having the concentration ranging from 0.1 to 1 mg. The adsorption profile is shown in Fig. 11. The trend of mucin adsorption was found to be in the following order Chitosan > DDS > Drug. The free drug molecules show no apparent adhering property towards mucin even at high concentration. In the case of chitosan and DDS, % of adsorption was found to be increased with increase in the amount of mucin added.

Chitosan was already reported as a first generation mucoadhesive material, because of the presence of NH_2 groups (cationic behaviour). So it can be easily adsorbed by the negatively charged mucous layer at the physiological conditions. The DDS also shows better adsorption percentage. It was reported that the negatively charged composite can also exhibits the mucous adsorption through H-bonding, hydrophobic interactions and vander Waals interaction which can be regulated by the pH.

Polymeric amphiphiles can form self assembled nanoparticles in an aqueous environment through hydrophobic interac-

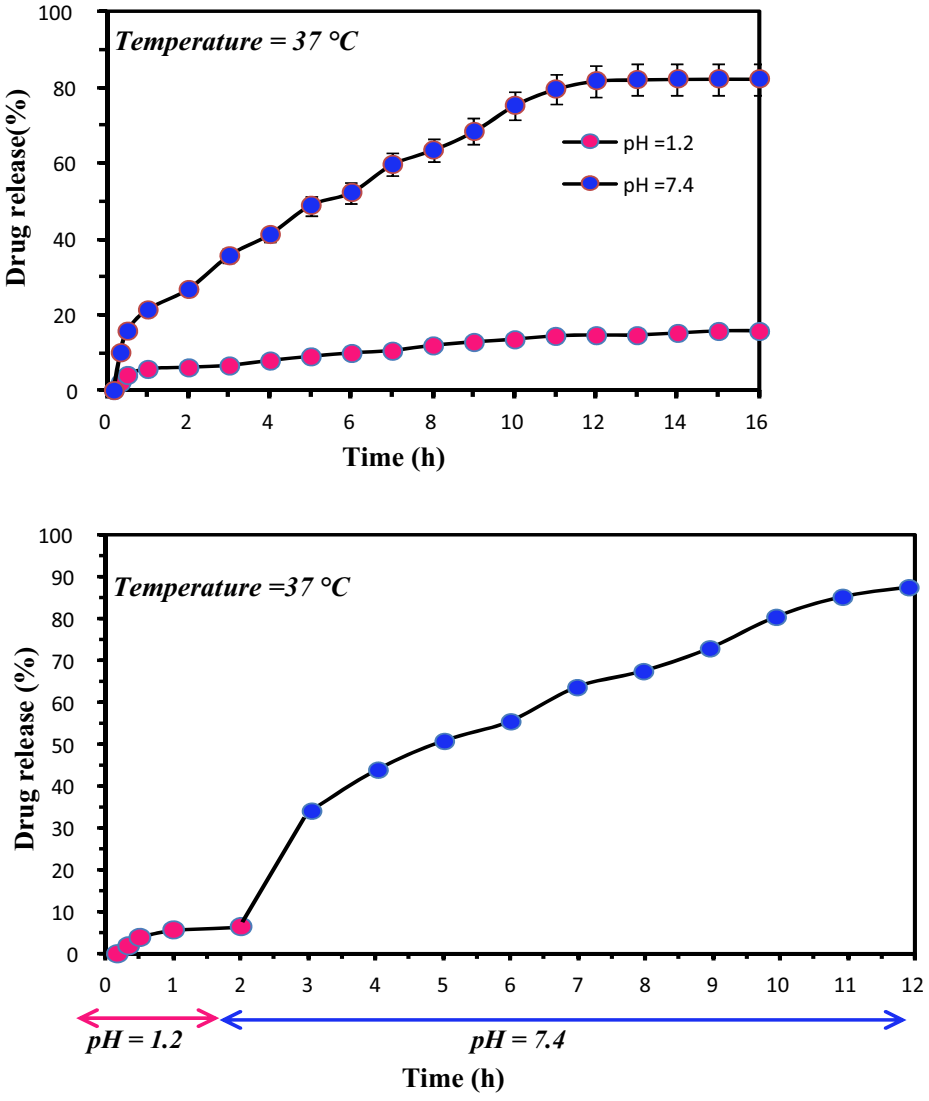

Fig. 10 The in vitro release profile at pH 1.2 and 7.4.

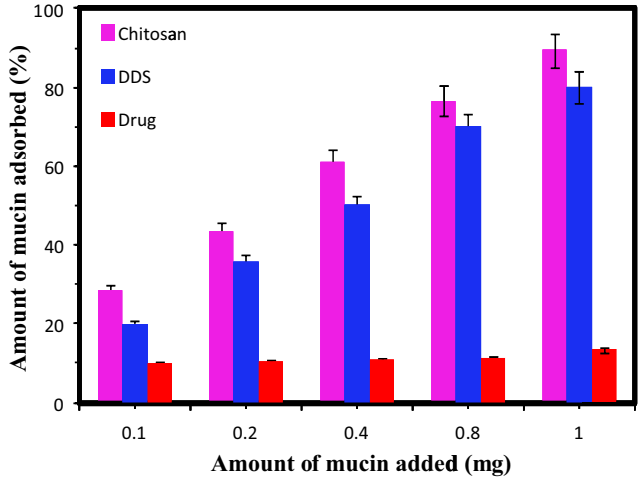

Fig. 11 Mucin adsorption study.

tions between the hydrophobic parts to minimise interfacial free energy. Chitosan is a polysaccharide showing hydrophilic and cationic nature can form self assembled nanoparticles by attaching the hydrophobic moiety to the backbone of chitosan and its derivatives. These assemblies can be readily precipitated in a biological solution (pH 7.4). Therefore water soluble chitosan assemblies can be readily used for the development of DDS. Table 3 depicts the various chitosan based DDS developed for the controlled and targeted delivery of therapeutics.

3.10. Biocompatibility assay

The cytotoxicity assay was carried out in cancerous cell line of Human colorectal Adenocarcinoma cells (DLD1). The assay was carried out using the DDS and the drug loaded DDS for different concentration levels of 6.25, 12.5, 25, 50 and 100 μg/mL. The % of cell viability of the drug delivery system was found to be better (greater than 50%) even at high concentration, indicates the non-toxicity and safety of the materials for biological applications (Silva et al., 2013). But the cell via-

Table 3 Hydrophilic chitosan derivatives for drug delivery.

Material	Drug	Nature of composite	Nature of drug release	Reference
Chitosan-MMT	Aceclofenac	Intercalation	Sustained	Thakur et al., 2016a
Triphenyl-(chloro acetylated chitosan) phosphonium salt MMT	Ibuprofen	Intercalation	Sustained	Abdeen and Salahuddin, 2013
Chitosan/MMT Theophylline &	Paracetamol	Intercalation	Sustained	Cojocariu et al., 2012
Quaternized chitosan/MMT	BSA	Intercalation	Sustained	Wang et al., 2008
Chitosan-MMT composite	Curcumin	Intercalation	Sustained	Thakur et al., 2016b
Chitosan-MMT	Oxy tetracycline	Intercalation	Controlled	Salcedo et al., 2014
2-Acrylamido-2-methyl propane sulphonic acid grafted N-Maleoyl chitosan-MMT	5-Flurouracil	Intercalation	Controlled	Anirudhan and Sandeep, 2011
N-Succinyl chitosan intercalated -MMT / grafted with acrylamide.	Paclitaxel	Intercalation	Controlled	Present study

bility of the drug loaded drug delivery system was showing significant decrease (Fig. 12). This was due to the successful participation of the anti-cancerous molecule present in the DDS. The morphology of the cell line after the MTT assay is shown in Fig. 13.

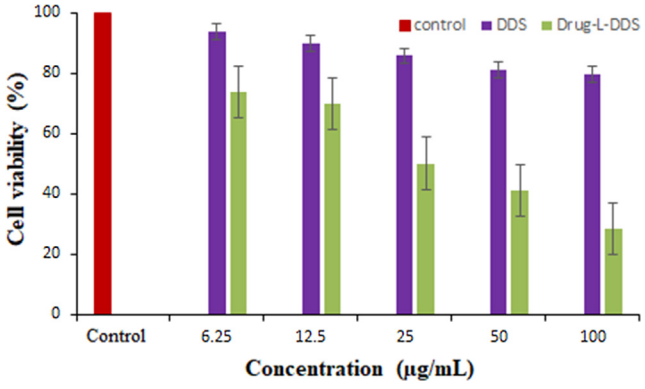

Fig. 12 The percentage of cell viability of the DDS and PTX-L-DDS in DLD1 cell line.

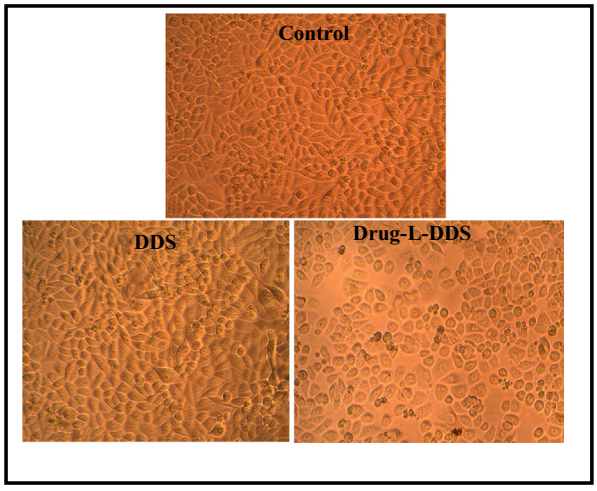

Fig. 13 Morphological images of DLD1 cell line treated with 6.25 µg/mL of DDS, Drug-L-DDS and Control.

3.11. Apoptosis study

The acquired images after live dead assay suggest that the cells when treated with our material of interest exhibit much more apoptosis tendency as compared to the untreated control. The cells showed a higher degree of stress and apoptosis induction after the material treatment. The control population showed green nucleus as they are healthy, but higher percentage of treated population showed orange stain with condensed chromatin suggesting it to be in the late apoptotic phase. Some cells also show green nucleus with condensation of chromatin, which points towards early apoptotic phase. This qualitative data clearly indicates that our material induces apoptosis in the cancer cells.

3.12. Flow cytometry

To find out whether the cells are directed to apoptosis or necrosis, a LIVE-DEAD assay was carried out. The flow cytometry is a quantitative study has been done to find out the change of DNA synthesis happening in the treated versus the untreated cells. DNA synthesis is one of the main characters of any actively dividing cells. The amount of DNA in the S -phase and G_2-M phase will be higher than G_0 phase for a healthy cell. More DNA content in the S phase indicate that the cell was actively planning to divide and same is the case of more DNA content in the G2-M phase. So in principle if a cell is damaged or stressed due any exogenous factor the cell, as a preventive mechanism, will enter in to the G_0 phase where it will try to repair the damage caused. So higher the DNA content in the G_0 phase indicates higher DNA damage.

So from the present study, it could be seen that the DNA content of S-phase and G_2-M phase in the treated cell population is lower than from the untreated ones. And also the cells which are treated showed higher percentage of DNA in the G_0 phase compared to the untreated. So this clearly indicates that the material of interest which we are using induces a considerable amount of DNA damage in the DLD1 cells in such a way that the cells retire from the normal division phase to the cell senescence phase. This DNA damage caused by our material is producing enough stress in the cells so that it may end up the cells getting into apoptosis phase. The results of apoptosis assay and the LIVE-DEAD assay is shown in Fig. 14.

4. Conclusion

An increasing number of nanostructured materials have been utilized for the delivery of various therapeutics. Polyacrylamide grafted succinyl chitosan intercalated bentonite (AAm-g-NB/SC) was prepared as a drug carrier system for the controlled delivery of paclitaxel. This was synthesized by combining the copolymer of succinyl chitosan intercalated bentonite and acrylamide using EGDMA as the crosslinking agent. The composite was characterized by FTIR, XRD, SEM, and thermal analysis. The DLS analysis showed that after the drug loading the particle size of the drug delivery system have a noticeable increase from 168.6 nm to 202 nm. Three different pH of 1.2, 6.8 and 7.4 were taken for the swelling studies in order to mimic the gastric and intestinal pH conditions. Among these three selected pH conditions, the maximum swelling was found to be occurring at the intestinal pH conditions. The release kinetics is controlled by both the diffusion and swelling process. The fitting of kinetic model was analysed at pH 7.4 and the release kinetics was found to be more fitted to Peppas kinetic model. The cytotoxicity assay was carried out in cancerous cell line of Human colorectal Adenocarcinoma cells (DLD1). The assay was carried out using the DDS and the drug loaded DDS for different concentration levels of 6.25, 12.5, 25, 50 and 100 μg/mL. The % of cell viability of the drug delivery system was found to be greater than 50% even at high concentration showing the non-toxicity and safety of the materials for biological applications. To find out whether the cells are directed to apoptosis or necrosis, a flow cytometry assay was carried out. Results

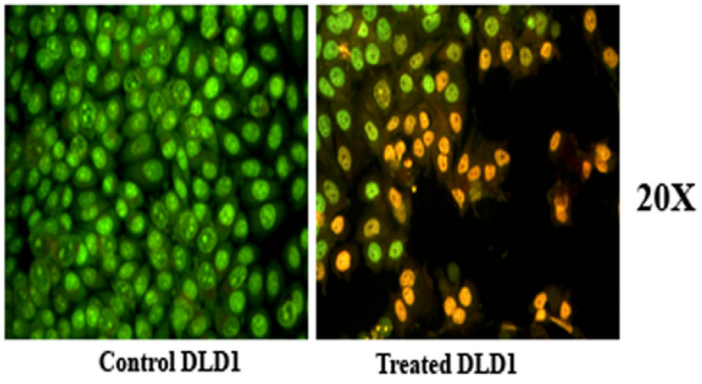

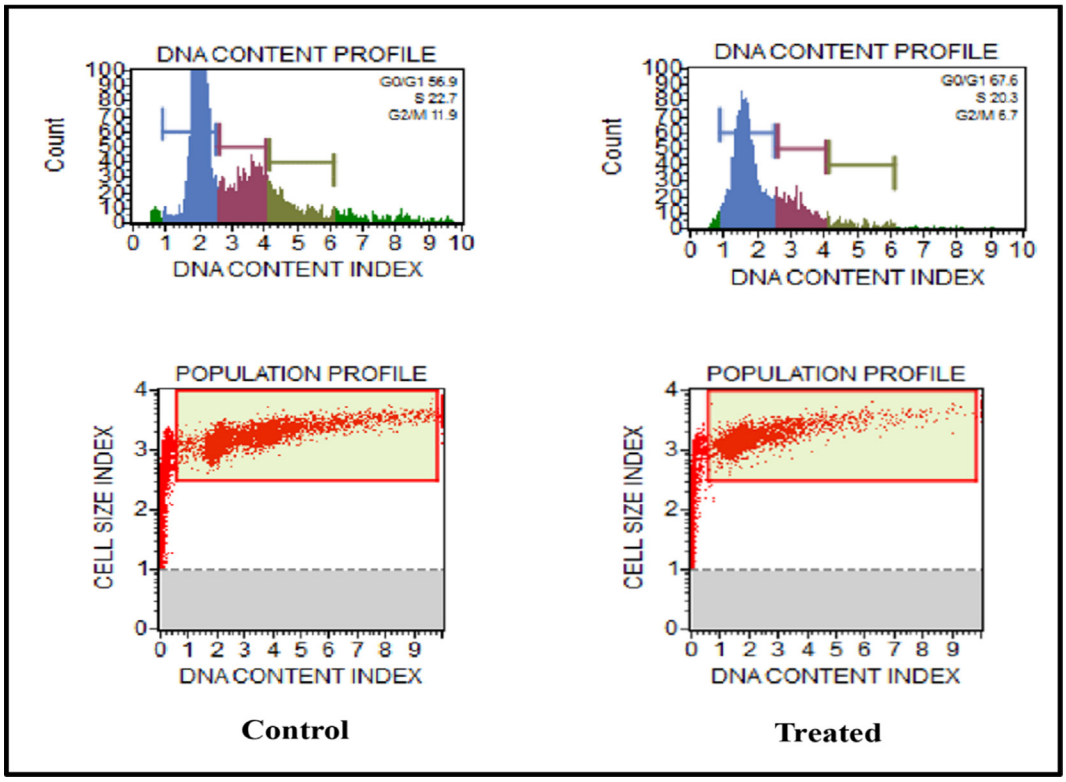

Fig. 14 Images of apoptosis on DLD1 of Control & PTX-L-DDS and the live-dead assay.

clearly indicates that the DDS induces a considerable amount of DNA damage in the DLD1 cells in such a way that the cells retire from the normal division phase to the cell senescence phase. On the whole, AAm-g-NB/SC developed in the present study can be effectively utilised for the controlled and targeted delivery of paclitaxel for the colorectal cancer therapy.

Acknowledgments

The authors are expressing sincere gratitude to The Head, Department of Chemistry, Fatima Mata National College, Kollam for providing laboratory facilities. The corresponding author thanks UGC, New Delhi for financial assistance in the form of Minor Research Project (2324-MRP/15-16/KLKE015/UGC-SWRO). The authors sincerely acknowledging the services rendered by Indian Institute of Science, Bangalore for their assistance in the characterization of the samples.

References

Abdeen, R., Salahuddin, N., 2013. Modified Chitosan-Clay Nanocomposite as a Drug Delivery System Intercalation and In Vitro Release of Ibuprofen. J. Chem., 1–9

Abral, H., Basri, A., Muhammad, F., Fernando, Y., Ha, F., Mahardika, M., Sugiarti, E., Sapuan, S.M., Ilyas, R.A., Stephane, I., 2019. Food Hydrocolloids A simple method for improving the properties of the sago starch fi lms prepared by using ultrasonication treatment 93, 276–283. https://doi.org/10.1016/j.foodhyd.2019.02.012.

Ahmad, R., Mohd, S., Ibrahim, R., Abral, H., Roslim, M., Huzaifah, M., Mohd, A., Murat, A., Azammi, N., Adrinata, M., Nor, M., Norrrahim, F., Jumaidin, R., 2019. Sugar palm (Arenga pinnata (Wurmb.) Merr) cellulosic fibre hierarchy : a comprehensive approach from macro to nano scale. Integr. Med. Res. 8, 2753–2766. https://doi.org/10.1016/j.jmrt.2019.04.011.

Akat, H., Tasdelen, M.A., Prez, F.Du., Yagci, Y., 2008. Synthesis and characterization of polymer/clay nanocomposites by intercalated chain transfer agent. Eur. Polym. J. 44, 1949–1954. https://doi.org/10.1016/j.eurpolymj.2008.04.018.

Amidon, S., Brown, J.E., Dave, V.S., 2015. Colon-Targeted Oral Drug Delivery Systems: Design Trends and Approaches. AAPS PharmSciTech 16, 731–741. https://doi.org/10.1208/s12249-015-0350-9.

Anirudhan, T.S., Sandeep, S., 2011. Synthesis and characterization of a novel pH-controllable composite hydrogel for anticancer drug delivery. New J. Chem. 35, 2869. https://doi.org/10.1039/c1nj20672a.

Asgari, M., Abouelmagd, A., Sundararaj, U., 2017. Silane functionalization of sodium montmorillonite nanoclay and its effect on rheological and mechanical properties of HDPE/clay nanocomposites. Appl. Clay Sci. 146, 439–448. https://doi.org/10.1016/j.clay.2017.06.035.

Aycan, D., Alemdar, N., 2018. Development of pH-responsive chitosan-based hydrogel modified with bone ash for controlled release of amoxicillin. Carbohydr. Polym. 184, 401–407. https://doi.org/10.1016/j.carbpol.2017.12.023.

Bertuoli, P.T., Piazza, D., Scienza, L.C., Zattera, A.J., 2014. Preparation and characterization of montmorillonite modified with 3-aminopropyltriethoxysilane. Appl. Clay Sci. 87, 46–51. https://doi.org/10.1016/j.clay.2013.11.020.

Cojocariu, A., Lenuta, P., Cheaburu, C., Cornelia, V., 2012. Chitosan / Montmorillonite Composites As Matrices for Prolonged Delivery of Some Novel Nitric Oxide Donor Compounds Based on Theophylline and Paracetamol. Cellul. Chem. Technol. 46, 35–43.

Dinakar, Y.H., 2018. Mucoadhesive Means of Drug Delivery – An Appraise. AJPS. 4, 21–28.

Feng, C., Li, J., Kong, M., Liu, Y., Cheng, X.J., Li, Y., Park, H.J., Chen, X.G., 2015. Surface charge effect on mucoadhesion of chitosan based nanogels for local anti-colorectal cancer drug delivery. Colloids Surfaces B Biointerfaces. 128, 439–447. https://doi.org/10.1016/j.colsurfb.2015.02.042.

Golyshev, A.A., Moskalenko, Y.E., Skorik, Y.A., 2015. Comparison of the acylation of chitosan with succinic anhydride in aqueous suspension and in solution. Russ. Chem. Bull. 64, 1168–1171. https://doi.org/10.1007/s11172-015-0994-3.

Halimatul, M.J., Sapuan, S.M., Jawaid, M., Ishak, M.R., Ilyas, R.A., 2019. Water absorption and water solubility properties of sago starch biopolymer composite films filled with sugar palm particles. Polimery. 64, 595–603.

He, H., Ma, L., Zhu, J., Frost, R.L., Theng, B.K.G., Bergaya, F., 2014. Synthesis of organoclays: a critical review and some unresolved issues. Appl. Clay Sci. 100, 22–28. https://doi.org/10.1016/j.clay.2014.02.008.

Helliwell, M., 1993. The use of bioadhesives in targeted delivery within the gastrointestinal tract. Adv. Drug Deliv. Rev. 11, 221–251. https://doi.org/10.1016/0169-409X(93)90011-R.

Ilyas, R.A., Ishak, M.R., Zainudin, E.S., 2018a. Akademia Baru Water Transport Properties of Bio-Nanocomposites Reinforced by Sugar Palm (Arenga Pinnata) Nanofibrillated Cellulose Akademia Baru 2, 234–246.

Ilyas, R.A., Sapuan, S.M., Ishak, M.R., Zainudin, E.S., 2018b. Development and characterization of sugar palm nanocrystalline cellulose reinforced sugar palm starch bionanocomposites. Carbohydr. Polym. https://doi.org/10.1016/j.carbpol.2018.09.002.

Jafarbeglou, M., Abdouss, M., Shoushtari, A.M., Jafarbeglou, M., 2016. Clay nanocomposites as engineered drug delivery systems. RSC Adv. 6, 50002–50016. https://doi.org/10.1039/c6ra03942a.

Khan, S., 2019. Highly Porous pH-Responsive Carboxymethyl Chitosan- Grafted -Poly (Acrylic Acid) Based Smart Hydrogels for 5-Fluorouracil Controlled Delivery and Colon Targeting.

Kumar, S., Koh, J., 2012. Physiochemical, optical and biological activity of chitosan-chromone derivative for biomedical applications. Int. J. Mol. Sci. 13, 6102–6116. https://doi.org/10.3390/ijms13056102.

Li, P., Zhang, J., Wang, A., 2007. A novel N-succinylchitosan-graft-polyacrylamide/attapulgite composite hydrogel prepared through inverse suspension polymerization. Macromol. Mater. Eng. 292, 962–969. https://doi.org/10.1002/mame.200700081.

Mansa, R., Detellier, C., 2013. Preparation and characterization of guar-montmorillonite nanocomposites. Materials (Basel). 6, 5199–5216. https://doi.org/10.3390/ma6115199.

Martins, K.F., Messias, A.D., Leite, F.L., Duek, E.A.R., 2014. Preparation and characterization of paclitaxel-loaded PLDLA microspheres. Mater. Res. 17, 650–656. https://doi.org/10.1590/s1516-14392014005000028.

Mukhopadhyay, P., Sarkar, K., Bhattacharya, S., Bhattacharyya, A., Mishra, R., Kundu, P.P., 2014. PH sensitive N-succinyl chitosan grafted polyacrylamide hydrogel for oral insulin delivery. Carbohydr. Polym. 112, 627–637. https://doi.org/10.1016/j.carbpol.2014.06.045.

Mullassery, M.D., Fernandez, N.B., Surya, R., Thomas, D., 2018. Microwave- assisted green synthesis of acrylamide cyclodextrin-grafted silylated bentonite for the controlled delivery of tetracycline hydrochloride. Sustain. Chem. Pharm. 10, 103–111. https://doi.org/10.1016/j.scp.2018.10.006.

Niu, H., Chen, H., Wen, G., Feng, J., Zhang, Q., Wang, J., 2018. One-pot solvothermal synthesis of three-dimensional hollow PtCu alloyed dodecahedron nanoframes with excellent electrocatalytic performances for hydrogen evolution and oxygen reduction. J. Colloid Interface Sci. 539, 525–532. https://doi.org/10.1016/j.jcis.2018.12.066.

Niu, H., Wang, A., Zhang, L., Guo, J., Feng, J., 2019a. Ultrafine NiCoP-decorated N,S,P-codoped hierarchical porous carbon nanosheets as an efficient bifunctional electrocatalyst for oxygen

reduction and oxygen evolution .RSC. https://doi.org/10.1039/c9qm00385a.

Niu, H., Zhang, L., Feng, J., Zhang, Q., Huang, H., Wang, A., 2019b. Journal of Colloid and Interface Science Graphene-encapsulated cobalt nanoparticles embedded in porous nitrogen-doped graphitic carbon nanosheets as efficient electrocatalysts for oxygen reduction reaction. J. Colloid Interface Sci. 552, 744–751. https://doi.org/10.1016/j.jcis.2019.05.099.

Pourjavadi, A., Farhadpour, B., Seidi, F., 2008. Synthesis and Investigation of Swelling Behavior of Grafted Alginate / Alumina Superabsorbent. Starch. 60, 457–466. https://doi.org/10.1002/star.200800208.

Pourjavadi, A., Mahdavinia, G.R., 2006. Superabsorbency, pH-sensitivity and swelling kinetics of partially hydrolyzed chitosan-g-poly(acrylamide) hydrogels. Turkish J. Chem. 30, 595–608.

Rathee, P., Jain, M., Garg, A., Nanda, A., Hooda, A., 2011. Gastrointestinal mucoadhesive drug delivery system: a review. J. Pharm. Res. 4, 1448–1453.

Salcedo, I., Sandri, G., Aguzzi, C., Bonferoni, C., Cerezo, P., Sánchez-Espejo, R., Viseras, C., 2014. Intestinal permeability of oxytetracycline from chitosan-montmorillonite nanocomposites. Colloids Surfaces B Biointerfaces. 117, 441–448.

Shin, J.P.H., Hwan, M., Kim, K.J., Kang, N., Kim, J.L.K., Ike, J., Kim, D., 2016. Application of montmorillonite in bentonite as a pharmaceutical excipient in drug delivery systems. J. Pharm. Investig. https://doi.org/10.1007/s40005-016-0258-8.

Siepmann, J., Peppas, N.A., 2012. Modeling of drug release from delivery systems based on hydroxypropyl methylcellulose (HPMC). Adv. Drug Deliv. Rev. 64, 163–174. https://doi.org/10.1016/j.addr.2012.09.028.

Silva, R.F., Araújo, D.R., Silva, E.R., Ando, R.A., Alves, W.A., 2013. L -Diphenylalanine microtubes as a potential drug-delivery system: Characterization, release kinetics, and cytotoxicity. Langmuir 29, 10205–10212. https://doi.org/10.1021/la4019162.

Sörensen, M.H., Samoshina, Y., Claesson, P.M., Alberius, P., 2009. Sustained release of ibuprofen from polyelectrolyte encapsulated mesoporous carriers. J. Dispers. Sci. Technol. 30, 892–902. https://doi.org/10.1080/01932690802644095.

Surya, R., Mullassery, M.D., Fernandez, N.B., Thomas, D., 2019. Journal of Science : Advanced Materials and Devices Synthesis and characterization of a clay-alginate nanocomposite for the controlled release of 5-Flurouracil. J. Sci. Adv. Mater. Devices 4, 432–441. https://doi.org/10.1016/j.jsamd.2019.08.001.

Tetsuka, H., Katayama, I., Sakuma, H., Tamura, K., 2018. Effects of humidity and interlayer cations on the frictional strength of montmorillonite. Earth, Planets Sp. 70, 1–9. https://doi.org/10.1186/s40623-018-0829-1.

Tiwari, G., Tiwari, R., Sriwastawa, B., Bhati, L., Pandey, S., Pandey, P., Bannerjee, S.K., 2012. Drug delivery systems: An updated review. Int. J. Pharm. Investig. 2, 2–11. https://doi.org/10.4103/2230-973X.96920.

Thakur, G., Singh, A., Singh, I., 2016a. Chitosan-montmorillonite polymer composites: Formulation and evaluation of sustained release tablets of aceclofenac. Sci. Pharm. 84, 603–617. https://doi.org/10.3390/scipharm8404060.

Thakur, G., Singh, A., Singh, I., 2016b. Formulation and evaluation of transdermal composite films of chitosan-montmorillonite for the delivery of curcumin. Int. J. Pharm. Investig. 6 (2016), 23.

Torres, M.A., Beppu, M.M., Santana, C.C., 2007. Characterization of chemically modified chitosan microspheres as adsorbents using standard proteins (bovine serum albumin and lysozyme). Brazilian J. Chem. Eng. 24, 325–336. https://doi.org/10.1590/S0104-66322007000300003.

Wang, X., Du, Y., Luo, J., 2008. Biopolymer/montmorillonite nanocomposite: preparation, drug-controlled release property and cytotoxicity. Nanotechnology 19. https://doi.org/10.1088/0957-4484/19/6/065707.

Yan, C., Chen, D., Gu, J., Hu, H., Zhao, X., Qiao, M., 2006. Preparation of *N*-Succinyl-chitosan and Their Physical-Chemical Properties as a Novel Excipient. Yakugaku Zasshi 126, 789–793. https://doi.org/10.1248/yakushi.126.789.